

Response to reviewer #2's comments

We would like to thank the reviewer for the positive reception of our work and constructive comments that helped us to improve our manuscript. In this document we provide our replies to the reviewer's comments. Page and line numbers in the responses correspond to those in the AMTD paper.

1. **Page 4, Line 7: How sensitive is the reagent ion intensity to the position of the corona needle?**

The position of the corona needle was chosen to obtain the maximum current of $\text{NH}_4^+(\text{H}_2\text{O})_n$ primary ions. Additional sensitivity tests have not been conducted.

2. **Page 4, Line 25: Is the 180 C for the air temperature of the thermal desorption region? Is this temperature prone to decompose labile molecules?**

We add the following sentence to the manuscript (P4 L25):

“For more details see the Supporting Information.”

We include the following discussion in the Supporting Information (P S1):

“In order to find the optimal temperature for the thermal desorption unit (TDU), we conduct a series of experiments with ammonia sulfate seeds coated with alpha-pinene ozonolysis products. We monitor the particle concentration after the thermal desorption unit using Scanning Mobility Particle Sizer Spectrometer (SMPS, TSI Incorporated) while increasing the temperature of TDU. The results are presented on Fig S1 below. The majority of particles is evaporated at temperatures above 140°C.

We study thermal decomposition of OVOCs extracted from alpha-pinene SOA by measuring their peak intensities using NH_4^+ -CIMS. Signals of many species increase at moderate temperatures ($T < 160^\circ\text{C}$) and level out or decrease at higher temperatures ($T > 180^\circ\text{C}$), as shown in Fig S2. Therefore, we choose the TDU temperature to be 180°C, as at this temperature all particles are evaporated while thermal decomposition of labile species is relatively small.

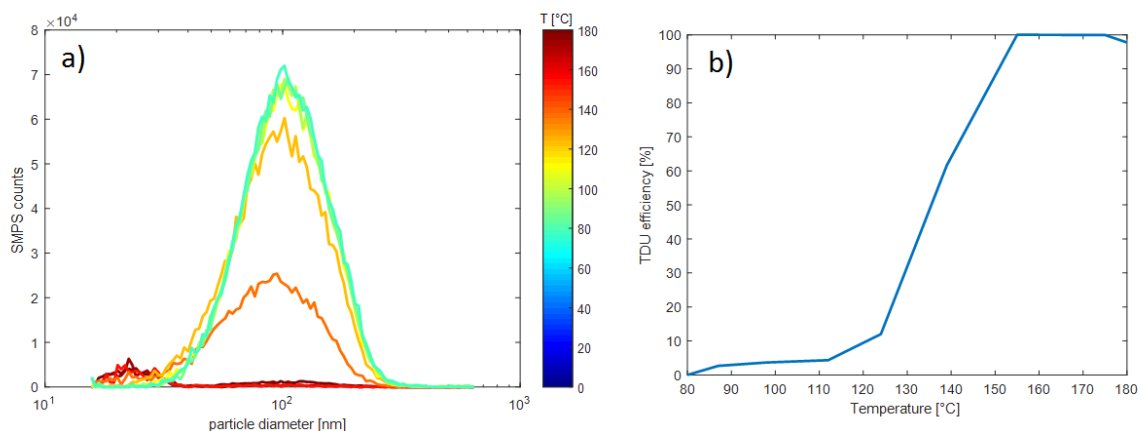


Figure S1: (a) Particle distribution measured by SMPS as a function of temperature of the thermal desorption unit of the NH_4^+ -CIMS; (b) Percentage of particles evaporated in the thermal desorption unit as a function of temperature of the unit.

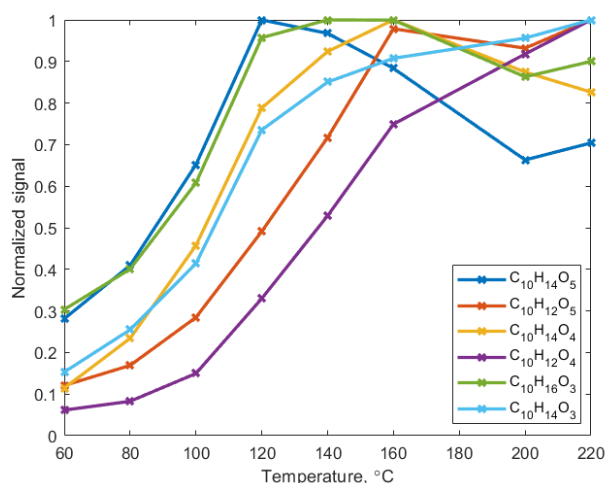


Figure S2: Thermograms of selected alpha-pinene ozonolysis SOA.

3. **Page 4, Line 26: How sensitive is the distribution of reagent ions in the NH_4^+ mode to the concentration of the ammonium hydroxide aqueous solution?**

We include the following discussion to the manuscript (P4 L8):

“For our setup, the concentration of the ammonium hydroxide aqueous solution of approximately 10% leads to an optimal $\text{NH}_4^+(\text{H}_2\text{O})_n$ primary ion signal with moderate impurities (Fig. S4). At smaller concentrations, excessive $\text{H}_3\text{O}^+(\text{H}_2\text{O})_n$ primary ions are produced, while at higher concentrations $\text{NH}_4^+(\text{NH}_3)$ becomes more prominent.”

4. **Page 5, Line 15: This is not exactly the case, as methanol exhibits relatively weaker dependence on humidity than pyruvic acid, biacetyl, and acetone. Is the humidity dependence related to the polarity of the analyte?**

Connection between the dipole moment and the sensitivity dependence on RH is relatively weak ($R^2=0.31$).

We modify the last two sentences of the section 3 of the manuscript (P5 L15):

“Generally, a stronger humidity dependence is observed for components with lower sensitivities at dry conditions. Higher molecular weight molecules have weaker humidity dependence. Humidity dependence of sensitivity does not show a strong correlation to cluster stability, as quantified by $\text{KE}_{50\text{ cm}}$ ($R^2 = 0.29$, Fig. S6). In addition, correlation between humidity dependence of sensitivity and polarity of analyte molecules is relatively weak ($R^2 = 0.31$).”

We include the following figure in the Supporting Information (Fig. S6, SI P8):

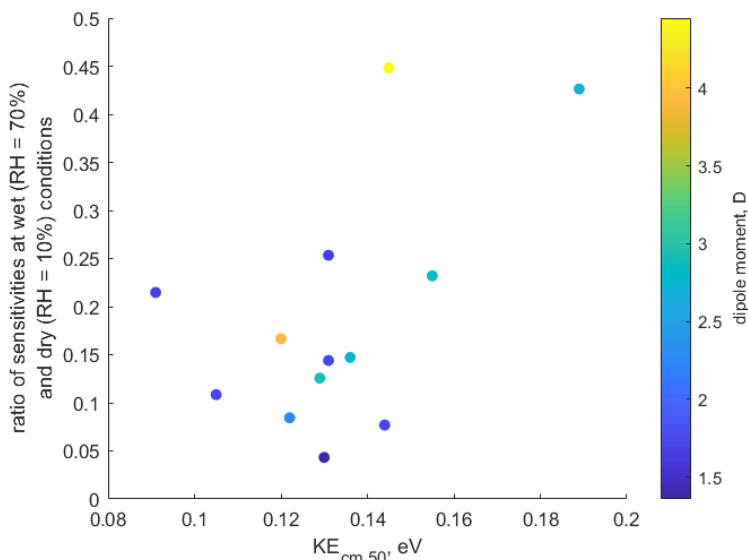


Figure S6: The relationship between the NH_4^+ -CIMS sensitivity dependence on RH and $\text{KE}_{\text{cm } 50}$. Data points are color-coded using the permanent dipole moment of the species.

5. **Page 5, Line 21: Increasing the analyte and reagent reaction time usually enhances the instrument sensitivity, which may not be simply the case for this study, as it could possibly promote the reverse ligand-switching reactions. Do the authors have any idea on the ideal reaction time in the ionization chamber?**

The product of the reaction time and the pressure in the reaction chamber defines the maximum volume mixing ratio of all VOCs which can be measured without depleting the primary ions (for a given ion-molecule reaction rate, e.g., $k=3 \cdot 10^{-9} \text{ cm}^3 \text{ s}^{-1}$). The instrument presented in this manuscript is designed for detecting the total VOC volume mixing ratio of 50 ppbv without significant depletion of primary ions.

The following description of how the reaction time was estimated is included in the paper (P6 L31):

“We calculate this limit by using experimentally-determined pressure and reaction time in the reaction chamber, and kinetic limit of ion-molecule reaction rate. We estimate the reaction time in the reaction chamber using the instrument sensitivity to specific compounds in the H_3O^+ mode. For polar compounds with proton affinity much higher than of water (i.e., acetone), we can assume that reverse proton transfer reactions do not occur. In this case, the instrument sensitivity to those compounds is given by (Lindinger et al., 1997):

$$\frac{i(\text{RH}^+)}{[\text{R}]} = i_{\text{primary}} \cdot k \cdot t_{\text{react}} \cdot \frac{p_{\text{react}}}{1013 \text{ mbar}} \quad (9)$$

where $\frac{i(\text{RH}^+)}{[\text{R}]}$ is the component sensitivity, i_{primary} is the primary ion current, k is the rate constant for the proton-transfer reaction (e.g., $k=3.6 \cdot 10^{-9} \text{ cm}^3 \text{ s}^{-1}$ for acetone, Cappellin et al., 2012), t_{react} and p_{react} are the reaction time and pressure in the reaction chamber, respectively.

By measuring the instrument sensitivity to acetone in the H_3O^+ mode, we estimate t_{react} to be 3 ms.”

6. **Page 6, Line 20: For some relatively big molecules such as decanone, their intensities increase with increasing de-clustering voltage. Please explain.**

Increasing the voltage between the ionization region and vacuum region of the mass-spectrometer leads to two opposite effects: 1) the ammonia-organic clusters are better guided to the vacuum region which results in higher transmission efficiency; 2) the clusters start breaking apart due to the increased collisional kinetic energy. Therefore, for very stable clusters we expect their signals to slightly increase at moderate voltages due to the higher transmission efficiency.

7. **Page 6, Line 30: How did the author take account for the influence of mass-dependent ion transmission through the ion optics on the ion signals?**

In order to compensate for the mass-dependent transmission of the ToF mass-spectrometer, we calculated the instrument sensitivities in duty cycle corrected counts per second ($\text{dcps}(i) = \text{cps}(i) \cdot \sqrt{100/m_i}$). Retrieved transmission efficiency is shown in Fig R4 (Holzinger et al., 2019):

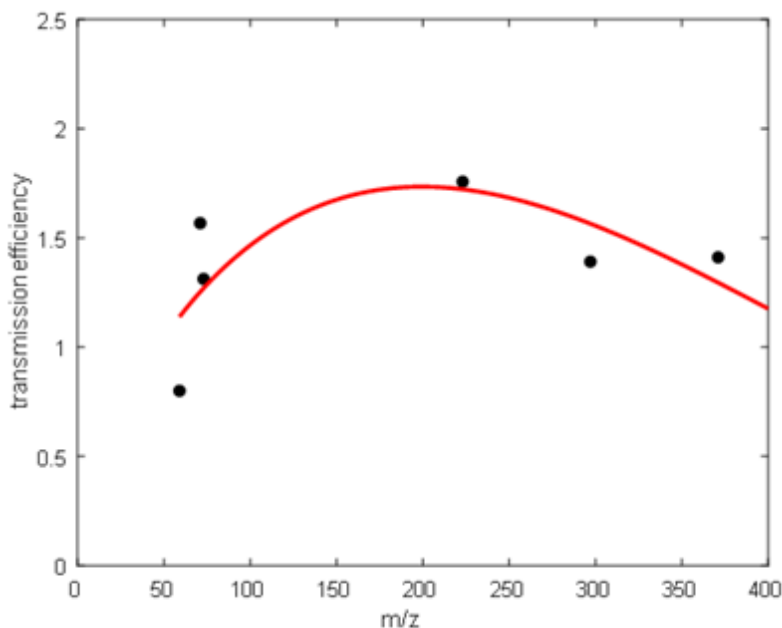


Figure R4: Retrieved transmission efficiency. The black dots correspond to transmission efficiency of acetone, methyl vinyl ketone, butanone, d3-, d4- and d5-siloxanes.

8. **Page 7, Line 15: Please provide the full mass spectra of all the ions detected, and compare the mass spectra of species in the gas phase with the particle-phase measurements in terms of peak identity and intensity.**

We include the following sentence to the manuscript (P7 L15):

“High-resolution mass-spectra of 3-methylcatechol oxidation products derived in the NH_4^+ -mode in the gas and particle phases are given in Fig S8.”

We include the following figure in the Supporting Information (Fig. S8, SI P10):

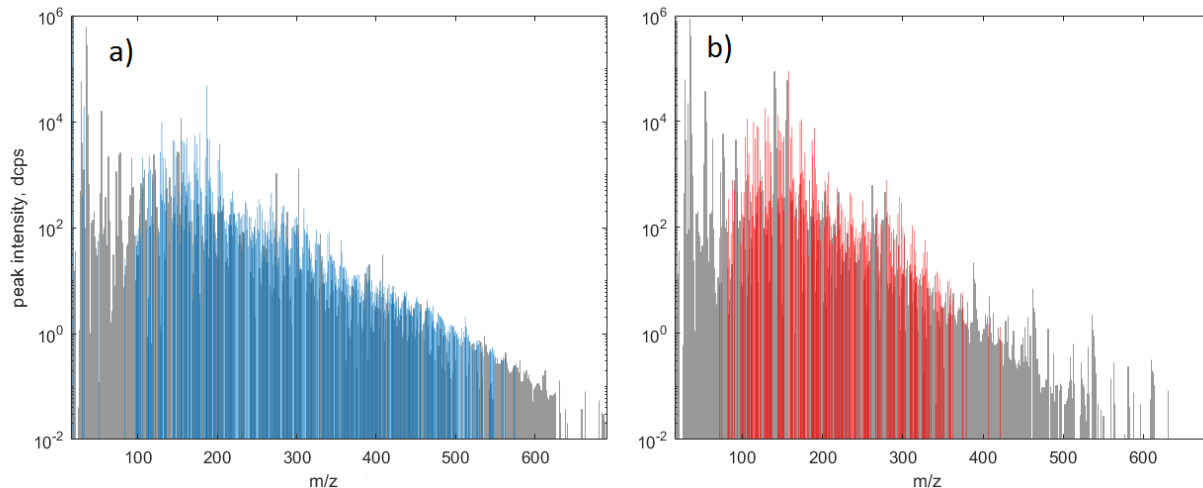


Figure S8: High-resolution mass-spectra obtained during photooxidation of 3-methylcatechol in (a) gas and (b) particle phases. Highlighted peaks are the ones that are enhanced during the experiment.

Fig R3 shows the mass defects of identified peaks in both gas and particle modes. In the mass defect plot, the blue, red, and yellow open circles represent the products observed in one or both modes and their signal is proportional to the logarithm of the signal intensity of observed clusters. Generally, heavier molecules are detected solely in the particle phase and lighter molecules entirely in the gas phase with the significant overlap in the medium range of masses.

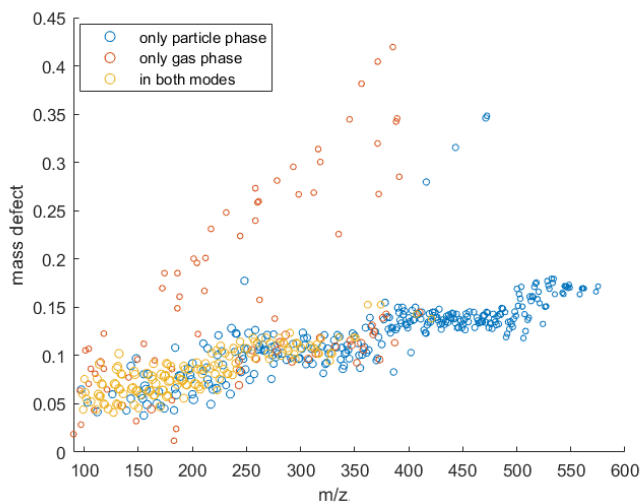


Figure R3: Comparison of mass-defect plots derived in the NH_4^+ mode for the gas and particle phase photooxidation products of 3-methylcatechol. The size of dots is proportional to the logarithm of the signal intensity of the observed clusters.

9. **Page 7, Line 20: This is a bit surprising, as the sensitivities of many species are largely different from that of acetone in PTR. But on the other hand, the comparison of the mixing ratios of organic compounds detected by both modes shows good agreement. Please evaluate uncertainties in applying a single sensitivity derived from acetone to all the OVOCs detected in the experiment.**

We include to the following discussion about the instrument sensitivity in the H_3O^+ mode (P7 L20):

“Breitenlechner et al. (2017) showed that due to the enhanced reaction time and the increased pressure in the reaction chamber the equilibrium between the forward and reverse proton reactions can be achieved. Hence, many compounds require careful calibration over a broad humidity range. Since PTR3 has the highest detected sensitivity to ketones, we use the acetone sensitivity to calculate the lower limit concentration of OVOCs.”

10. **Page 7, Line 25: As the NH_4^+ mode is able to detect larger and more functionalized molecules, how did the authors quantify the losses of these molecules in the CIMS inlet?**

Low volatile organic compounds (LVOC) have low saturation vapour pressure such that almost every collision with wall inlet leads to a complete loss. However, the estimates for these losses in the literature have shown significant discrepancy. Breitenlechner et al. (2017) estimated the wall losses for LVOC with more than five oxygens in the PTR3 inlet to be 80% while for VOC with less than five oxygens the wall losses were assumed to be negligible. Hansel et al. (2018) evaluated the wall losses in the CI3-ToF inlet to be 50%. Since we did not have another instrument with calibrated diffusion losses in the inlet (i.e., acetate-CIMS), we did not take into account wall losses of less volatile species in the instrument inlet. It results in underestimation of concentration of these molecules and can be one of the reasons of the difference between AMS and NH_4^+ -CIMS signals shown in Fig. 8.

The following sentence is modified (P7 L32):

“This discrepancy can be explained by a combination of the following factors: 1) uncertainties in the sensitivities obtained using the presented technique and in the AMS measurements; 2) thermal fragmentation of organic molecules in the thermal desorption unit which leads to lower observed masses in the mass spectrum; 3) low NH_4^+ -CIMS sensitivity to certain compounds of organic aerosols if ligand switching reactions between these molecules and ammonium-water clusters are endothermic (e.g., small organic acids); 4) wall losses of less volatile organic molecules in the NH_4^+ -CIMS inlet.”

11. **Page 12, Table 1: In addition to alcohols, carbonyls, and acids, is the NH_4^+ mode capable of detecting other species, like peroxides?**

NH_4^+ -CIMS is capable of detecting other species such as isoprene hydroxy hydroperoxide (ISOPOOH) and isoprene epoxydiols (IEPOX). Figure R4 shows the mass-spectra obtained during calibration of trans-IEPOX in both modes of the instrument. In the NH_4^+ mode, trans-IEPOX is

detected as $C_5H_{10}O_3 \cdot NH_4^+$ (m/z 136.0974) cluster with very little fragmentation. On the contrary, the signal of the protonated ion $C_5H_{10}O_3 \cdot H^+$ (m/z 119.0708) is relatively small while we observe significant fragmentation. Two most prominent fragments are $C_5H_8O_2 \cdot H^+$ (m/z 101.0603) and $C_4H_8O_2 \cdot H^+$ (m/z 89.0603).

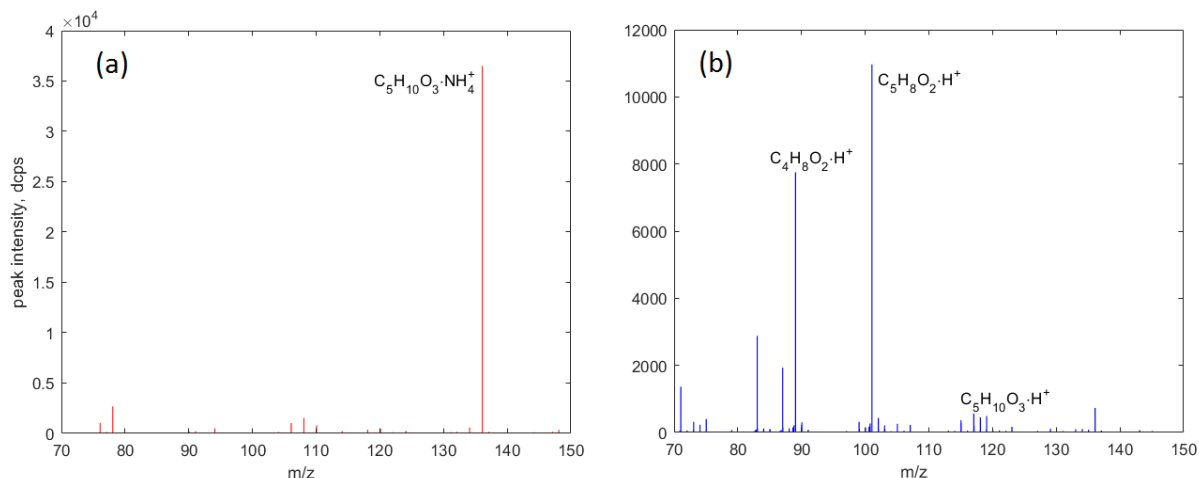


Figure R4: High-resolution mass-spectra obtained during calibration of trans-IEPOX in (a) NH_4^+ and (b) H_3O^+ modes.

References:

Breitenlechner, M., Fischer, M., Hainer, M., Heinritzi, M., Curtius, M., and Hansel, A.: PTR3: An instrument for Studying the Lifecycle of Reactive Organic Carbon in the Atmosphere, *Anal. Chem.*, 89, 5824–5831, doi:10.1021/acs.analchem.6bo5110, 2017.

Cappellin, L., Karl, T., Probst, M., Ismailova, O., Winkler, P. M., Soukoulis, C., Aprea, E., Märk, T.D., Gasperi, F., Biasioli, F.: On Quantitative Determination of Volatile Organic Compound Concentrations Using Proton Transfer Reaction Time-of-Flight Mass Spectrometry, *Environ. Sci. Technol.*, 46 (4), 2283–2290, doi: 10.1021/es203985t, 2012.

Hansel, A., Scholz, W., Mentler, B., Fischer, L., and Berndt, T.: Detection of RO2 radicals and other products from cyclohexene ozonolysis with NH_4^+ and acetate ionization mass spectrometry, *Atmos. Env.*, 186, 248–255, doi:10.1016/j.atmosenv.2018.04.023, 2018.

Holzinger, R., Acton, W. J. F., Bloss, W. J., Breitenlechner, M., Crilley, L. R., Dusanter, S., Gonin, M., Gros, V., Keutsch, F. N., Kiendler-Scharr, A., Kramer, L. J., Krechmer, J. E., Languille, B., Locoge, N., Lopez-Hilfiker, F., Materić, D., Moreno, S., Nemitz, E., Quéléver, L. L. J., Sarda Esteve, R., Sauvage, S., Schallhart, S., Sommariva, R., Tillmann, R., Wedel, S., Worton, D. R., Xu, K., and Zaytsev, A.: Validity and limitations of simple reaction kinetics to calculate concentrations of organic compounds from ion counts in PTR-MS, *Atmos. Meas. Tech. Discuss.*, <https://doi.org/10.5194/amt-2018-446>, in review, 2019.